

# Error Probability Optimization for Non-Orthogonal Multiple Access in DBMC Networks

Alexander Wietfeld, *Graduate Student Member, IEEE*, Sebastian Schmidt, *Graduate Student Member, IEEE*, Wolfgang Kellerer, *Senior Member, IEEE*

**Abstract**—Non-orthogonal multiple access (NOMA) represents a promising option for differentiating multiple transmitters using only a single molecule type in a future diffusion-based molecular communication (DBMC) network. This paper addresses the bit error probability optimization of a DBMC-NOMA network with bio-nano-machines incapable of complex computations for classical optimization methods. We propose a pilot-symbol-based algorithm to approximate the optimal detection threshold and emitted number of transmitter molecules. Our solution is based on two algorithms for the separate optimization of thresholds and the number of molecules, which are applied alternately. Our Monte-Carlo simulation results show that the algorithm reliably approaches the global optimum parameter values regardless of initial values and signaling-molecule-to-noise ratio. Since it is composed of only a few basic operations, such as comparisons and additions, there is potential for an implementation using stochastic chemical reaction networks in future work.

**Index Terms**—Molecular communication, non-orthogonal multiple access, optimization, heuristic algorithm, error probability

## I. INTRODUCTION

**D**IFFUSION-BASED molecular communication (DBMC) is envisioned to play a significant role in nanoscale and biological communication networks due to its advantages over electromagnetic communication with respect to biocompatibility, size constraints, and energy efficiency. To enable complex use cases such as targeted drug delivery and other advanced medical applications in a future internet of bio-nano-things (IoBNT) [1], bio-nano-machines (BNMs) must be able to cooperate and communicate. Individual BNMs are expected to perform only simple tasks such as emission of and reaction to surrounding molecules [1]. One step towards the communication between a large number of BNMs is enabling multiple access (MA). Multiple approaches to MA for DBMC have been investigated, such as time-division multiple access (TDMA), molecule-division multiple access (MDMA), and non-orthogonal multiple access (NOMA). NOMA based on successive interference cancellation (SIC) was recently proposed as an option for DBMC networks [2]. The motivation to explore NOMA stems both from its use of only a single

molecule type, limiting transmitter (TX) and receiver (RX) complexity, and the option for all TXs to transmit simultaneously, increasing capacity [3]. TDMA and MDMA each lack one of these two capabilities, simultaneous transmissions and single-molecule-type operation, respectively.

DBMC-NOMA was shown to match the performance of orthogonal schemes like MDMA for the optimal choice of communication parameters [3]. Therefore, optimizing the system to achieve the lowest possible bit error probability (BEP) is crucial, but in [3], only an exhaustive search of the analytical formula was considered.

On top of the potential advantages mentioned above, NOMA is connected to several shortcomings and added complexities. In [3], the need for an exponential increase in the emitted number of molecules, as the number of TXs grows, is highlighted. Additionally, NOMA can only work in the case of appropriate implementation and optimization of the SIC procedure to separate the TXs at the RX, which could be difficult in the highly constrained biological MC systems. Especially the latter issue will be addressed in this work. The optimization of parameters is relevant for various types of communication schemes. NOMA simply is a prescient example, due to its reliance on an optimized number of emitted molecules to operate, which we showed in [3].

Related work on parameter optimization for DBMC networks exists, for example, focused on analytical solutions [4], using global optimization algorithms like gradient descent optimization [5], or data-driven machine learning (ML) approaches [6]. While these methods reliably achieve the optimum value, they could be infeasible in an IoBNT framework, where we have to optimize parameters on low-capability BNMs. Stochastic chemical reaction networks have been proposed to capture the resulting constraints on possible computation procedures in DBMC systems more accurately, and implement simple heuristic methods based on pilot symbols and thresholds [7].

In this paper, we propose a pilot-symbol-based heuristic optimization algorithm targeted towards the BEP minimization in a DBMC network using NOMA. In contrast to previous work on NOMA for DBMC in [2], [3] that assumes accurate channel estimation to facilitate SIC, we frame the SIC procedure as threshold detection with multiple thresholds per TX. This allows for simple systematic optimization without explicit channel estimation. The presented algorithm alternately adjusts the detection threshold and emitted number of molecules per TX across multiple iterations based on decision rules derived from the mechanisms behind NOMA in a DBMC

Manuscript received April 29, 2024; accepted June 21, 2024.

The authors acknowledge the financial support by the Federal Ministry of Education and Research of Germany in the program of “Souverän. Digital. Vernetzt.”. Joint project 6G-life, project identification number: 16KISK002.

Alexander Wietfeld (e-mail: alexander.wietfeld@tum.de) and Wolfgang Kellerer (e-mail: wolfgang.kellerer@tum.de) are with the Chair of Communication Networks, Technical University of Munich, Germany.

Sebastian Schmidt was with the Chair of Communication Networks, Technical University of Munich, Germany, until March 2024 (e-mail: sebastian.a.schmidt@tum.de).

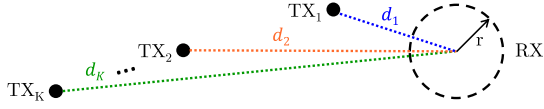


Fig. 1. DBMC scenario with  $K$  point transmitters at distances  $d_1, d_2 \dots d_K$  from a spherical receiver.

network found in [3]. The algorithm works without any knowledge of initial values or the underlying analytical function and its derivatives as opposed to analytical or gradient descent methods in previous work [4], [5]. Additionally, considering the limited capabilities of future BNMs, the algorithm uses only elementary operations as opposed to ML methods, which rely on large computational power [6]. We investigate the convergence of the algorithm for different choices of initial values and different levels of background noise. Lastly, we investigate its robustness to changes in channel conditions during run-time.

## II. SYSTEM MODEL

Figure 1 depicts a communication scenario with  $K$  TXs TX <sub>$i$</sub>  at distances  $d_1 \leq d_2 \leq \dots \leq d_K$  from a central spherical, passive RX with radius  $r$ . The TXs are modeled as points emitting instantaneous pulses of molecules. The received signal  $n_{RX}(t)$  is the number of molecules within the RX volume at time  $t$ . With  $N_{TX,i}$ , the number of molecules emitted by TX <sub>$i$</sub>  per pulse,  $V_{RX}$ , the RX volume, and the diffusion coefficient  $D$ , the impulse response between one TX <sub>$i$</sub>  and the RX can be modeled as a Poisson-distributed random variable  $n_{RX}(t) \sim \mathcal{P}(\lambda_i(t))$  [8] with time-varying mean

$$\lambda_i(t) = \frac{N_{TX,i} V_{RX}}{(4\pi Dt)^{\frac{3}{2}}} \exp\left(-\frac{d_i^2}{4Dt}\right). \quad (1)$$

Eq. (1) is valid under the uniform concentration assumption [8], and if  $n_{RX}(t)$  is sufficiently small in comparison to a sufficiently large  $N_{TX,i}$  [9]. If additionally  $\lambda_i(t)$  is sufficiently large, the received signal can be further approximated by a Gaussian distribution  $n_{RX}(t) \sim \mathcal{N}(\mu_i, \sigma_i^2)$  with mean  $\mu_i(t) = \lambda_i(t)$  and variance  $\sigma_i^2(t) = \lambda_i(t)$  [9].

The TXs use on-off-keying (OOK), where a pulse of  $N_{TX,i}$  molecules is emitted for a '1' and nothing for a '0' with both symbols equally likely. The emitted number of molecules is limited by a maximum molecule budget  $N_{TX,max}$  per symbol per TX. We assume that the system is fully synchronized and that the symbol period  $T$  is sufficiently large such that inter-symbol interference (ISI) is negligible. Therefore, we consider only the current symbol, where all TX <sub>$i$</sub>  send a pulse of  $s_i N_{TX,i}$  molecules at  $t = 0$ , with the symbol from TX <sub>$i$</sub>  denoted by  $s_i \in \{0, 1\}$ . For decoding, the RX takes one sample per time slot at the peak time  $t_p$  of the received signal.

In this paper, we implement the DBMC-NOMA scheme described in [3]. Therefore, with respect to the current time slot, all TXs transmit simultaneously using the same molecule type. The overall received signal at  $t_p$  is a sum of multiple independent random variables. For Poisson and Gaussian variables, the sum can be modeled as a single distribution with combined mean and variance  $\lambda_{NOMA} = \lambda_n + \sum_{i=1}^K s_i \lambda_i(t_p)$ , where  $\lambda_i(t_p)$  represents the expected value of the contribution

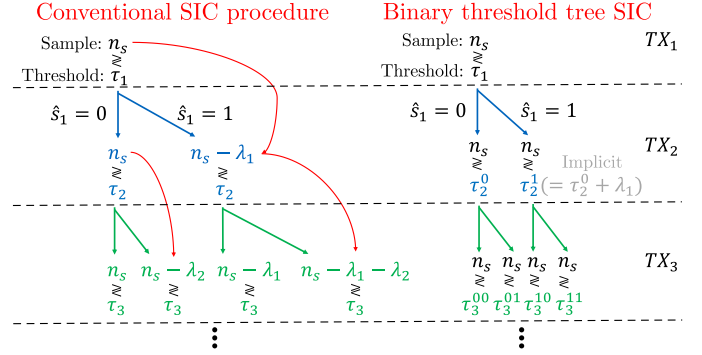


Fig. 2. Diagram on the left shows the conventional description of the SIC procedure based on subtracting the estimated component from TX <sub>$i$</sub> ,  $\lambda_i$ , from the sample. Equivalent procedure shown on the right using a set of thresholds  $\tau_i^s$  for each TX resulting in a binary tree structure for comparing the same sample  $n_s$  multiple times.

from TX <sub>$i$</sub>  and  $\lambda_n$  is an additive noise term. The sample at the RX is a realization of the distribution  $n_s \sim \mathcal{P}(\lambda_{NOMA})$  or  $n_s \sim \mathcal{N}(\lambda_{NOMA}, \lambda_{NOMA})$ .

### A. Successive Interference Cancellation

To differentiate the symbols from each TX <sub>$i$</sub>  at the RX, successive interference cancellation (SIC) and simple detection with thresholds  $\tau_i$  is used. The detected symbol for TX <sub>$i$</sub>  is denoted as  $\hat{s}_i$ . TXs are considered for detection by the RX one by one from TX<sub>1</sub> to TX<sub>K</sub>. We note, that through optimization of the emitted number of molecules, the TXs will tend towards an order from large to small expected signal contribution  $\lambda_i(t_p)$ . Usually, for NOMA in classical communications as well as for DBMC, it is assumed that the contribution of the currently considered TX to the received signal is removed from the sample value  $n_s$  after each detection using channel estimation information about each TX's  $\lambda_i(t_p)$  [3]. For example, after comparing  $n_s$  to  $\tau_1$  and detecting  $\hat{s}_1 = 1$ , the sample is adjusted to  $n_s - \lambda_1(t_p)$  before detecting the symbol from TX<sub>2</sub>, as depicted on the left side of Figure 2.

In this paper, we propose to model SIC as threshold detection with multiple thresholds per TX instead. To detect the symbol sent by TX <sub>$i$</sub> , the RX employs threshold detection on the sample  $n_s$  with the decision rule

$$\hat{s}_i = \begin{cases} 1 & n_s \geq \tau_i^{\hat{s}_{i-1}} \\ 0 & n_s < \tau_i^{\hat{s}_{i-1}} \end{cases}, \quad (2)$$

where  $\hat{s}_{i-1} = [\hat{s}_1, \dots, \hat{s}_{i-1}]$  is the vector of all previously detected symbols for the TXs up to and including TX <sub>$i-1$</sub> . Thereby, we end up with a set  $\mathcal{T}_i = \{\tau_i^{0\dots000}, \tau_i^{0\dots001}, \tau_i^{0\dots010}, \dots, \tau_i^{1\dots110}, \tau_i^{1\dots111}\}$  of  $2^{i-1}$  different possible thresholds for TX <sub>$i$</sub> . The procedure is depicted on the right side of Figure 2 and compared to the conventional model. Under our assumptions of threshold detection and OOK, the two are exactly equivalent, if we set  $\tau_2^1 = \tau_2^0 + \lambda_1$  and similarly for the other thresholds. Generally, the second model gives us the opportunity to freely optimize the set of thresholds  $\mathcal{T}_i$  without explicit channel estimation.

### B. Evaluation Metric

We will evaluate the performance of the network using the system bit error probability (BEP), i.e., the average BEP across

all TXs, denoted as  $P_{e,\text{sys}} = \frac{1}{K} \sum_{i=1}^K P_{e,i}$ , with the individual BEP of TX<sub>*i*</sub>,  $P_{e,i}$ . For the sake of the scalability of our Monte Carlo simulations (MCSs), we approximate the Poisson distribution with the Gaussian as described at the beginning of the section. Otherwise, the calculations are based on the derivation in [3] and adapted for the specific assumptions in this paper. We offer a detailed calculation of  $P_{e,i}$  in the supplementary appendix. The final BEP expression incorporates multiple access interference, which is a crucial aspect for the DBMC-NOMA system with simultaneously transmitting TXs. To introduce the notion of channel quality, we use the signaling-molecule-to-noise ratio (SNR):  $\text{SNR} = \frac{\max_i \lambda_i(t_p)}{\lambda_n}$ . The SNR is later used as an input value to the evaluation representing the additive noise  $\lambda_n$ .

### III. PILOT-SYMBOL-BASED BEP OPTIMIZATION

The BEP of a DBMC-NOMA system depends on many different parameters. The detection thresholds and the emitted number of molecules from each TX are two primary factors due to their effect on the detection performance and the received number of molecules, respectively, as shown in [3]. Therefore, we will also focus on the optimal choice of detection thresholds  $\mathcal{T}_i^*$  and the emitted number of molecules  $N_{\text{TX},i}^*$ , i.e., attempting to solve the optimization problem

$$\begin{aligned} \{\mathcal{T}_i^*, N_{\text{TX},i}^*\}_{i=1}^K &= \arg \min_{\{\mathcal{T}_i, N_{\text{TX},i}\}_{i=1}^K} P_{e,\text{sys}} \quad (3) \\ \text{s.t. } N_{\text{TX},i} &\leq N_{\text{TX},\text{max}} \forall i \in [1, \dots, K]. \end{aligned}$$

Analytical solutions and global optimization algorithms [3]–[5] often lead to the optimal values. However, these methods require capabilities from the nodes in the network, such as accurate channel estimation, storage of pre-computed solutions, or computation of functions or their derivatives, for example, for a gradient descent algorithm. Compared to the current and even future capabilities of synthetic cells that will act as BNMs in DBMC networks, these tasks are very complex. Therefore, we aim to find possibly greedy heuristics that rely on simpler operations<sup>1</sup>. Previously, pilot-symbol-based approaches have been shown to work together with stochastic chemical reaction networks to approximate a real-world implementation of DBMC using simple operations like threshold comparisons [7].

To approximate a solution of Eq. (3), we propose pilot-symbol-based optimization algorithms, first separately for the detection thresholds and the number of molecules. Ultimately, we combine the two for a joint optimization of the BEP in a DBMC-NOMA system. In the following, for the sake of brevity and simplicity of the depicted algorithms, we will assume a network with 2 TXs, i.e.,  $K = 2$ .

#### A. Optimizing the Detection Thresholds

For the design of the algorithm optimizing the detection thresholds, we assume that the number of molecules  $N_{\text{TX},i}$  is

<sup>1</sup>We note, that convexity of the objective function is an important property for global algorithms and heuristic schemes alike. In line with the extensive but inconclusive discussion of BEP convexity in MC systems in [5], a proof of convexity of  $P_{e,\text{sys}}$  is beyond the scope of this paper, but remains as a crucial topic of investigation.

static. The scheme is based on a sequence of pilot symbols from  $\mathcal{S}_{\text{pilot}} = \{\mathbf{s} = [s_1 s_2]; s_j \in \{0, 1\}\}$ , which is known to both TXs and the RX. As with the DBMC-NOMA scheme, all symbols in each pilot symbol vector  $\mathbf{s}$  are sent simultaneously from all TXs. Starting from a set of initial values  $[\tau_{1,\text{init}}, \tau_{2,\text{init}}, \tau_{2,\text{init}}^1]$ , the thresholds are adjusted after the transmission, sampling, and decoding of a pilot symbol  $\mathbf{s}$  as defined in Section II. The detected symbols are then compared to the correct symbols in the pilot sequence. If the symbol is detected correctly, the threshold stays the same. If the symbol is incorrectly detected as a '1', the threshold is increased to make the detection of a '0' more likely. Consequently, the threshold is decreased for a symbol incorrectly detected as '0'. Note that for a certain pilot symbol vector  $\mathbf{s}$ , only the applicable threshold is altered for TX<sub>2</sub>, for example,  $\tau_2^1$  in the case  $s_1 = 1$ . Importantly, we apply  $\tau_2^{s_1}$  for the detection of  $\hat{s}_2$  based on the pilot symbol  $s_1$ , not the detected symbol  $\hat{s}_1$ . Thereby, for the purposes of the threshold optimization, we assume correct detection for all previous TXs. The scheme is described in detail in Algorithm 1.

#### Algorithm 1 Detection Threshold Optimization Algorithm

---

```

INPUT:  $\tau_1, \tau_2^0, \tau_2^1$ 
for  $i = 1$  to  $N_{\text{pilot}}$  do
  CHOOSE:  $\mathbf{s} \leftarrow [s_1, s_2] \in \mathcal{S}_{\text{pilot}}$ 
  TRANSMIT: TX1  $\rightarrow s_1 N_{\text{TX},1}$ , TX2  $\rightarrow s_2 N_{\text{TX},2}$ 
  RECEIVE:  $n_s \leftarrow n_{\text{RX}}(t_p) \sim \mathcal{N}(\lambda_{\text{NOMA}}, \lambda_{\text{NOMA}})$ 
  DECODE TX1: Use  $\tau_1$  to obtain  $\hat{s}_1$ , Eq. (2)
  if  $\hat{s}_1 \neq s_1$  AND  $s_1 = 0$  then
    |  $\tau_1 \leftarrow \tau_1 + \Delta\tau$ 
  else if  $\hat{s}_1 \neq s_1$  AND  $s_1 = 1$  then
    |  $\tau_1 \leftarrow \tau_1 - \Delta\tau$ 
  DECODE TX2: Use  $\tau_2^{s_1}$  to obtain  $\hat{s}_2$ , Eq. (2)
  if  $\hat{s}_2 \neq s_2$  AND  $s_2 = 0$  then
    |  $\tau_2^{s_1} \leftarrow \tau_2^{s_1} + \Delta\tau$ 
  else if  $\hat{s}_2 \neq s_2$  AND  $s_2 = 1$  then
    |  $\tau_2^{s_1} \leftarrow \tau_2^{s_1} - \Delta\tau$ 
OUTPUT:  $\tau_1, \tau_2^0, \tau_2^1$ 

```

---

#### B. Optimizing the Emitted Number of Molecules

Similarly to Algorithm 1, we now assume that the detection thresholds are static and the number of molecules is adjusted based on the transmission, sampling, and decoding of a pilot sequence known to both TXs and RX. Here, one TX is randomly assigned  $N_{\text{TX},\text{max}}$  by the RX and denoted as TX<sub>1</sub>. As a result, it is possible to assign the maximum molecule budget per TX  $N_{\text{TX},\text{max}}$  as  $N_{\text{TX},1}$  and focus on optimizing  $N_{\text{TX},2}$  relative to that maximum starting from an initial value  $N_{\text{TX},\text{init}}$ . This works as long as the TXs distances are sufficiently similar and the RX can send the change in  $N_{\text{TX},2}$  to the correct TX, as discussed later for the feedback mechanism.

After detecting the symbols from both TXs, we propose to use a set of decision rules determining the adjustment of  $N_{\text{TX},2}$ . Firstly, there is only a reason for changing  $N_{\text{TX},2}$ , if  $s_2 = 1$ . Otherwise it stays the same. If  $s_2 = 1$ , we will now describe two example cases to illustrate the rationale behind the decision rules. If  $\hat{s}_1 \neq s_1 = 0$ , and  $\hat{s}_2 = s_2 = 1$ , this means that we should decrease  $N_{\text{TX},2}$  since we observed enough molecules to classify  $s_2 = 1$ , but there were too many molecules such that we incorrectly crossed the threshold for TX<sub>1</sub>. If  $\hat{s}_1 = s_1 = 0$ , and  $\hat{s}_2 \neq s_2 = 1$ , it means that we should

increase  $N_{TX,2}$  since we incorrectly did not observe enough molecules to cross the threshold for TX<sub>2</sub>, but the detection for TX<sub>1</sub> is still not affected by too much interference from TX<sub>2</sub>. For adapting  $N_{TX,2}$ , we utilize a multiplicative model, i.e.,  $N_{TX,2} \leftarrow N_{TX,2} \cdot (1 \pm \alpha_N)$ , with the number of molecules multiplier  $\alpha_N$ .

Additionally, there is a feedback mechanism from the RX back to TX<sub>2</sub> to communicate the necessary adjustment, for example, via a separate control signaling molecule, which we do not model in detail. The RX communicates two pieces of information back to the TXs: which TX is targeted, and how should this TX adapt  $N_{TX,i}$ . We assume that this would be encoded via orthogonal binary sequences and decoded via correlation, and that therefore, a binary erasure channel with either correct detection or loss of information is appropriate. In case an adaptation to  $N_{TX,2}$  is sent from the RX side, the subsequent change to  $N_{TX,2}$  at TX<sub>2</sub> is modeled by

$$N_{TX,2} \leftarrow \begin{cases} N_{TX,2} & \text{with prob. } p_{e,f} \\ N_{TX,2} \cdot (1 \pm \alpha_N) & \text{else} \end{cases}, \quad (4)$$

with the feedback erasure probability  $p_{e,f}$ . If not otherwise specified, we set  $p_{e,f} = 0$ . More details of the optimization scheme can be found in Algorithm 2.

### Algorithm 2 Number of Molecules Optimization Algorithm

```

INPUT:  $N_{TX,2}$ 
for  $i = 1$  to  $N_{\text{pilot}}$  do
  CHOOSE:  $\mathbf{s} \leftarrow [s_1, s_2] \in \mathcal{S}_{\text{pilot}}$ 
  TRANSMIT: TX1  $\rightarrow s_1 N_{TX,1}$ , TX2  $\rightarrow s_2 N_{TX,2}$ 
  RECEIVE:  $n_s \leftarrow n_{RX}(t_p) \sim \mathcal{N}(\lambda_{\text{NOMA}}, \lambda_{\text{NOMA}})$ 
  DECODE TX1: Use  $\tau_1$  to obtain  $\hat{s}_1$ , Eq. (2)
  DECODE TX2: Use  $\tau_2^1$  to obtain  $\hat{s}_2$ , Eq. (2)
  if  $s_2 = 1$  then
    if  $s_1 = 0$  AND  $\hat{s}_1 \neq s_1$  AND  $\hat{s}_2 = s_2$  then
       $N_{TX,2} \leftarrow N_{TX,2} \cdot (1 - \alpha_N)$  with probability  $1 - p_{e,f}$ 
    if [ $s_1 = 0$  AND  $\hat{s}_1 = s_1$  AND  $\hat{s}_2 \neq s_2$ ]
      OR [ $s_1 = 1$  AND  $\hat{s}_1 \neq s_1$  AND  $\hat{s}_2 \neq s_2$ ]
      OR [ $s_1 = 1$  AND  $\hat{s}_1 = s_1$  AND  $\hat{s}_2 \neq s_2$ ] then
         $N_{TX,2} \leftarrow N_{TX,2} \cdot (1 + \alpha_N)$  with probability  $1 - p_{e,f}$ 
OUTPUT:  $N_{TX,2}$ 

```

### C. Alternating Joint Optimization Algorithm

Given Algorithm 1 and Algorithm 2, we need either knowledge of the optimal number of molecules or detection thresholds, respectively, to arrive at the joint optimal solution. Therefore, we propose a joint BEP optimization scheme based on alternating between Algorithms 1 and 2 using arbitrary initial values for both detection thresholds and number of molecules. Both partial optimization algorithms are run once for  $N_{\text{pilot}}$  pilot symbols, and this is repeated for  $N_{\text{iter}}$  iterations. After each set of pilot symbols, the threshold output of Algorithm 1 is used as the input for Algorithm 2 to optimize the number of molecules and vice-versa.

## IV. NUMERICAL RESULTS

In the following, the proposed algorithm will be evaluated using Monte Carlo simulations (MCSs) based on the Gaussian stochastic channel model described in Section II. The optimization process with  $N_{\text{iter}}$  iterations of the joint algorithm

TABLE I

Parameter	Symbol	Values (Default)
TX distances	$\{d_1, d_2\}$	$\{10, 11, 12\}$ $\mu\text{m}$
RX radius	$r$	1 $\mu\text{m}$
Diffusion coefficient	$D$	$10^{-9}$ $\text{m}^2 \text{s}^{-1}$
Signaling-molecule-to-noise ratio	SNR	$\{\infty, 3, 16\}$
Molecule budget per TX	$N_{TX,\text{max}}$	$10^6$ molecules
Number of pilot symbols	$N_{\text{pilot}}$	1000
Number of iterations	$N_{\text{iter}}$	1000
Threshold step	$\Delta\tau$	1 molecule
Number of molecules multiplier	$\alpha_N$	0.1
Initial thresholds	$\tau_{\text{init}}$	$[1, 1, 1]$ molecules
Initial number of molecules	$N_{TX,\text{init}}$	$\{1, 10^6\}$ molecules
Feedback erasure probability	$p_{e,f}$	$\{0, 0.5, 0.9, 0.99\}$

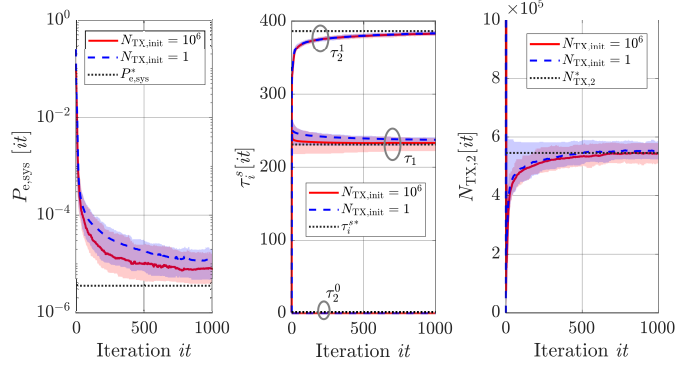


Fig. 3. Performance of the joint algorithm for two choices of initial value  $N_{TX,\text{init}}$ . Median (bold line) and 5th–95th percentile (shaded area) of bit error probability  $P_{e,\text{sys}}$ , detection thresholds  $\tau_i^s$ , and emitted number of molecules from TX<sub>2</sub>  $N_{TX,2}$  shown across 1000 iterations repeated 100 times.

in Section III-C is repeated 100 times. An overview of the simulation parameters can be found in Table I.

Firstly, Figure 3 depicts the development of all parameters for two choices of the initial number of molecules, either  $N_{TX,\text{init}} = 1$  or  $N_{TX,\text{init}} = N_{TX,\text{max}} = 10^6$ . The results show that the BEP is reliably optimized without any knowledge of the current or optimal BEP itself. There is a convergence towards the optimal parameters  $\tau_i^{s*}$ ,  $N_{TX,2}^*$  (obtained separately via exhaustive search) and therefore also the optimal BEP,  $P_{e,\text{sys}}^*$ . Additionally, the difference for an initial value at either end of the applicable spectrum is visible but does not disturb the overall convergence. This shows the robustness of the algorithm towards the choice of initial value. We also observe

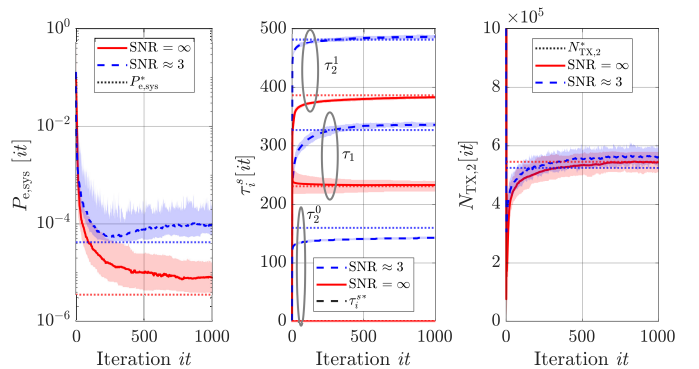


Fig. 4. Performance of the joint algorithm for two different values of SNR. Median (bold line) and 5th–95th percentile (shaded area) of bit error probability  $P_{e,\text{sys}}$ , detection thresholds  $\tau_i^s$ , and emitted number of molecules from TX<sub>2</sub>  $N_{TX,2}$  shown across 1000 iterations repeated 100 times.

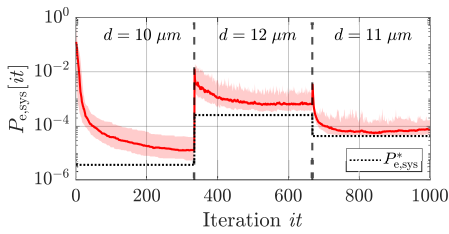


Fig. 5. Median (bold line) and 5th–95th percentile (shaded area) of bit error probability  $P_{e,sys}$  for 100 runs of 1000 iterations of the joint algorithm. After 333 and 666 iterations the distance of the TXs to the RX was changed from  $10 \mu\text{m}$  to  $12 \mu\text{m}$  and again to  $11 \mu\text{m}$ , respectively.

that when the thresholds and  $N_{TX,i}$  are far from the optimum at the beginning, there are a lot of errors and, therefore, a lot of adjustments to the values by the algorithm, causing more drastic changes, followed by smaller adjustments as we approach the optimum.

Secondly, in Figure 4, we also look at the performance of the algorithm under varying levels of background noise, comparing the results for  $\text{SNR} = \infty$  to  $\text{SNR} \approx 3$ . The plots show that the optimization also works for the case with noise. Crucially, the optimal values are significantly influenced by the added noise, but the algorithm approximates them without knowledge of the noise level. We can observe some increased variability and jitter in the median and percentiles, and it seems as if the algorithm slightly overestimates both the optimal threshold and the number of molecules for the case of added noise. A rigorous investigation of the underlying reasons is left for further work.

Figure 5 evaluates the reaction of the algorithm to changes in the channel conditions during run-time. The sequence of 1000 iterations is split into three parts, where after every 333 iterations, the distance of both TXs is changed from  $10 \mu\text{m}$  to  $12 \mu\text{m}$  and subsequently to  $11 \mu\text{m}$ . We can observe that although the instantaneous BEP jumps up at the time of the change, the subsequent speed of the optimization is quick. Especially for the first few iterations after the change, the BEP is reduced by orders of magnitude towards the optimum. This shows the potential of this type of algorithm to work in a running DBMC system.

Lastly, in Figure 6, the effect of the feedback channel model in Eq. (4) from the RX to  $\text{TX}_2$  is investigated. On the left side of the figure, several values of  $p_{e,f}$  are compared. Effects on the BEP only become visible for  $p_{e,f} \geq 50\%$  signifying robustness against feedback channel issues. While the overall trajectory and especially the immediate BEP reduction at the outset remain undisturbed even up to  $p_{e,f} = 99\%$ , the convergence becomes significantly slower and the resulting BEP after 1000 iterations is one order of magnitude worse. However, the right-hand-side of Figure 6 depicts the continuation of the algorithm for a further 2000 iterations at  $p_{e,f} = 99\%$ . We can clearly see that the BEP improvement continues towards the optimum, albeit much slower.

## V. CONCLUSION

In this paper, we proposed a BEP optimization algorithm for a DBMC network using NOMA based on the transmission of pilot symbols. We have shown that the algorithm can reliably

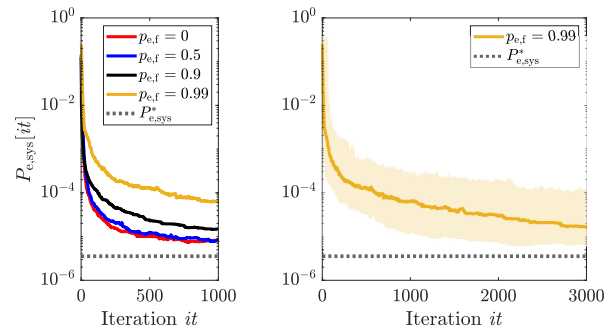


Fig. 6. Median bit error probability  $P_{e,sys}$  for 100 runs of the joint algorithm. Left side compares different values of the feedback erasure probability  $p_{e,f}$  over 1000 iterations. Right side depicts the case of  $p_{e,f} = 99\%$  for a continuation of the algorithm to 3000 iterations. Shaded area represents 5th–95th percentile.

approximate the optimal values for the detection threshold and the number of molecules in a system with 2 TXs and 1 RX, requiring no prior knowledge of the initial values. This provides a promising perspective for the use of MA schemes in a real MC network. Additionally, the algorithm deliberately uses simple steps without the computation of more complex functions. We plan to address the implementation of the algorithm using stochastic chemical reaction networks in future work. The promise of implementing such simple algorithms or even basic neural network structures [10] using chemical reactions could be the basis for many of the crucial IoBNT use cases including disease detection, classification, and targeted treatment inside an autonomous in-body network.

## REFERENCES

- [1] I. F. Akyildiz, M. Pierobon, S. Balasubramaniam, and Y. Koucheryavy, “The Internet of Bio-Nano Things,” *IEEE Commun. Mag.*, Mar. 2015.
- [2] A. Wietfeld, S. Schmidt, and W. Kellerer, “Non-Orthogonal Multiple Access for Diffusion-Based Molecular Communication Networks,” in *Proc. 10th ACM Int. Conf. Nanoscale Comput. Commun.*, (Coventry, UK), Sept. 2023. short paper, presented as poster.
- [3] A. Wietfeld, S. Schmidt, and W. Kellerer, “DBMC-NOMA: Evaluating NOMA for Diffusion-Based Molecular Communication Networks,” to appear in *Proc. IEEE Int. Conf. Commun. (ICC)*, June 2024.
- [4] L. Chouhan, P. K. Sharma, and N. Varshney, “Optimal Transmitted Molecules and Decision Threshold for Drift-Induced Diffusive Molecular Channel With Mobile Nanomachines,” *IEEE Trans. NanoBiosci.*, Oct. 2019.
- [5] Z. Cheng, Y. Tu, K. Chi, and M. Xia, “Optimization of Decision Thresholds in Two-Way Molecular Communication via Diffusion With Network Coding,” *IEEE Trans. Mol. Biol. Multi-Scale Commun.*, Dec. 2022.
- [6] X. Qian, M. Di Renzo, and A. Eckford, “Molecular Communications: Model-Based and Data-Driven Receiver Design and Optimization,” *IEEE Access*, Apr. 2019.
- [7] B. Heinlein, L. Brand, M. Egan, M. Schäfer, R. Schober, and S. Lotter, “Stochastic Chemical Reaction Networks for MAP Detection in Cellular Receivers,” in *Proc. 10th ACM Int. Conf. Nanoscale Comput. Commun.*, (Coventry, UK), Sept. 2023.
- [8] V. Jamali, A. Ahmadzadeh, W. Wicke, A. Noel, and R. Schober, “Channel Modeling for Diffusive Molecular Communication—A Tutorial Review,” *Proc. IEEE*, July 2019.
- [9] J. Torres Gómez, K. Pitke, L. Stratmann, and F. Dressler, “Age of information in molecular communication channels,” *Digital Signal Processing*, May 2022.
- [10] S. Angerbauer, W. Haselmayr, F. Enzenhofer, T. Pankratz, R. Khanzadeh, and A. Springer, “Molecular Nano Neural Networks (M3N): In-Body Intelligence for the IoBNT,” to appear in *Proc. IEEE Int. Conf. Commun. (ICC)*, June 2024.



**Alexander Wietfeld** (Graduate Student Member, IEEE) received the B.Sc. and M.Sc. degrees in electrical engineering with a focus on communication engineering from RWTH Aachen with distinction in 2021 and 2023, respectively. He is currently pursuing the Dr.-Ing. degree at the Chair of Communication Networks, Technical University of Munich. His research interests are in the fields of molecular communication networks and the internet of bio-nano-things, including work on multiple access techniques and resource optimization.



**Sebastian Schmidt** (Graduate Student Member, IEEE) received the B.Sc. and M.Sc. degrees in Electrical Engineering and Information Technology from the Technical University of Munich (TUM) in 2018 and 2022 respectively, with distinction. From 2023 to 2024 he was a graduate research assistant at the Chair of Communication Networks, TUM, where he worked on molecular communication networks and the internet of bio-nano things.



**Wolfgang Kellerer** (Senior Member, IEEE) is a Full Professor with the Technical University of Munich (TUM), Germany, heading the Chair of Communication Networks at the School of Computation, Information and Technology. He received his Ph.D. degree in Electrical Engineering from the same university in 2002. He was a visiting researcher at the Information Systems Laboratory of Stanford University, CA, US, in 2001. Prior to joining TUM, Wolfgang Kellerer pursued an industrial career, being for over ten years with NTT DOCOMO's European Research Laboratories. He was the director of the infrastructure research department, where he led various projects for wireless communication and mobile networking contributing to research and standardization of LTE-A and 5G technologies. In 2015, he has been awarded with an ERC Consolidator Grant from the European Commission for his research on flexibility in communication networks. He currently serves as an associate editor for IEEE Transactions on Network and Service Management and as the area editor for network virtualization for IEEE Communications Surveys and Tutorials.